THE MOVEMENT OF MEMBRANOUS ORGANELLES IN AXONS

Electron Microscopic Identification of Anterogradely and Retrogradely Transported Organelles

SHOICHIRO TSUKITA and HARUNORI ISHIKAWA

From the Department of Anatomy, University of Tokyo Faculty of Medicine, Hongo 7-3-1, Bunkyo-ku, Tokyo 113, Japan

ABSTRACT

To identify the structures to be rapidly transported through the axons, we developed a new method to permit local cooling of mouse saphenous nerves in situ without exposing them. By this method, both anterograde and retrograde transport were successfully interrupted, while the structural integrity of the nerves was well preserved. Using radioactive tracers, anterogradely transported proteins were shown to accumulate just proximal to the cooled site, and retrogradely transported proteins just distal to the cooled site. Where the anterogradely transported proteins accumulated, the vesiculotubular membranous structures increased in amount inside both myelinated and unmyelinated axons. Such accumulated membranous structures showed a relatively uniform diameter of 50–80 nm, and some of them seemed to be continuous with the axonal smooth endoplasmic reticulum (SER). Thick sections of nerves selectively stained for the axonal membranous structures revealed that the network of the axonal SER was also packed inside axons proximal to the cooled site. In contrast, large membranous bodies of varying sizes accumulated inside axons just distal to the cooled site, where the retrogradely transported proteins accumulated. These bodies were composed mainly of multivesicular bodies and lamellated membranous structures. When horseradish peroxidase was administered in the distal end of the nerve, membranous bodies showing this activity accumulated, together with unstained membranous bodies. Hence, we are led to propose that, besides mitochondria, the membranous components in the axon can be classified into two systems from the viewpoint of axonal transport: "axonal SER and vesiculotubular structures" in the anterograde direction and "large membranous bodies" in the retrograde direction.

KEY WORDS axonal transport · membrane transport · local cooling · saphenous nerve electron microscopy · radioactive tracer

The axonal transport system comprises fast anterograde, fast retrograde, and slow anterograde transport (for reviews, see 30, 37, 43, 50). Of these three types of axonal transport, slow anterograde transport has been recognized as a bulk movement of the axoplasm (31, 37, 46). Through the axoplasm, various materials are rapidly transported both anterogradely and retrogradely. This fast ax-

onal transport has been intensively investigated for a better understanding of the physiology and metabolism of the neuron, and the intracellular transport of materials in general. Although various models have been proposed to explain its mechanism (33, 48, 53), they are still speculative, mainly because of a lack of ultrastructural evidence.

In biochemical analysis of fast anterograde transport, the transport of proteins seemed to be associated mainly with "particulate" fractions (10, 14, 19, 32, 44, 49). The labeled phospholipids and proteins were found to be transported at the same rate, possibly in the form of membranes (1, 23). Electron microscopic autoradiographic studies revealed that rapidly transported proteins were related to the presence of membranous organelles, especially the axonal smooth endoplasmic reticulum (SER) (9, 15, 28, 54). Furthermore, it has been recently demonstrated that the axonal SER forms a well-developed continuous network in myelinated axons (16, 56). These studies strongly suggest that the axonal SER may participate in fast anterograde transport, but direct evidence is still lacking.

Retrograde axonal transport is also a well-known phenomenon. Discovery of retrograde transport of horseradish peroxidase (HRP) has prompted morphological analysis of this type of transport (35). The retrograde transport of HRP was cytochemically demonstrated in membranous organelles and small tubules within the axons (38, 39, 47, 55). Concerning the membranous structures involved in anterograde transport, the following questions arise: What kinds of membranous organelles participate in anterograde and retrograde transport? Is the axonal SER involved in both transports? Furthermore, recent demonstrations of anterograde transport of HRP in some nerves have made these problems more complex (11, 27, 38, 47, 52, 55). Hence, identification of membranous organelles involved in anterograde and retrograde transport is prerequisite to understanding their mechanism.

To know in what forms the materials are transported, the ligation or transection of nerves has been commonly used, and many observations have been made of the morphological changes at both sides of ligated or transected regions (42). However, the information obtained from such experiments was limited because it was difficult to distinguish the morphological changes caused by interruption of the transport from those due to local injury. Because low temperature blocks fast axonal transport (1, 13, 22, 25, 29, 51), local cooling has been successfully used to interrupt fast axonal transport for the biochemical analysis (8, 17, 26). We used this technique for morphological studies on excised nerves and on locally exposed nerves. Neither approach was satisfactory for morphological analysis, however, because of the difficulty of maintaining ultrastructural integrity. Previously, we studied mouse-tail nerves for ultrastructural analysis of anterograde transport, using a new local cooling method based on the principle that the nerve should not be exposed to any extent (57).

In the present study, a new local cooling method was developed for ultrastructural studies of both anterograde and retrograde transport, and by this new method we obtained evidence that indicates that membranous organelles indeed move inside axons in both directions and that the retrogradely transported organelles can be morphologically distinguished from the anterogradely transported organelles.

MATERIALS AND METHODS

Animals and Nerves

Saphenous nerves of male albino mice weighing 30–40 g were used in this study. The nerve is composed of peripheral branches of both L_2 and L_3 dorsal root ganglion cell axons. This nerve runs just beneath the skin along the leg after emerging from the deep muscular layer at the inguinal region.

Local Cooling Procedure

A mouse was confined on its back within a cardboard box, the limbs extended outside through four small holes. When the tip of each limb was fastened to the stage with vinyl tape, the mouse was hardly able to move its limbs. The hair on the right femoral region was shaved off with a razor blade and then the saphenous nerve running along the vessels was visible through the skin.

Two aluminum blocks were stuck together, with a thin layer of heat-insulating materials interposed. Each block had a U-shaped tunnel inside with two open exits, through which a warm or cold water-ethanol mixture was circulated to maintain the temperature of each block at 35° or 0°C. This aluminum device was fixed with instant adhesive to the hair-shaved skin exactly above the saphenous nerve (Fig. 1). When the warm block was placed proximal to the cold one, the proximal portion of the nerve was warmed and the distal portion was cooled to interrupt the anterograde transport. The warm block was used to focus the leading edge of the cooled area. Inversely, with the cold block proximal to the warm one, the proximal portion was cooled to interrupt the retrograde transport. After cooling, the nerve just beneath the heat-insulating materials was marked ("marked point").

Radioactive Tracer Experiment for Anterograde Transport

Under ether anesthesia, a right L_2 dorsal root ganglion was exposed by partial laminectomy, and L-[^{14}C]leucine (0.4 μCi in

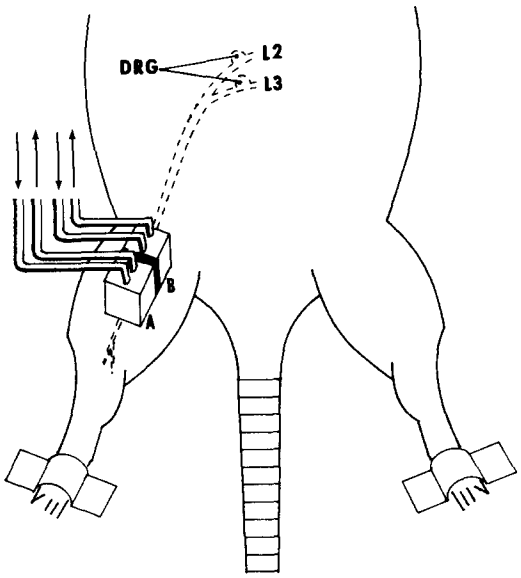

FIGURE 1 Schematic drawing of the local cooling method. The right saphenous nerve of an albino mouse originates in L_2 and L_3 dorsal root ganglia (*DRG*). This nerve runs just beneath the skin along the leg after emerging from the deep muscle layer at the inguinal region. After the hair on the right femoral region was shaved off, the aluminum apparatus was fixed with instant adhesive to the hair-shaved skin exactly above the saphenous nerve. The aluminum apparatus was composed of two aluminum blocks (*A*, 5 mm × 5 mm × 4 mm; *B*, 5 mm × 5 mm × 3 mm) which are stuck together, with a thin layer of heat-insulating material interposed. Each block has a U-shaped tunnel inside with two open exits, through which a cold or warm water-ethanol mixture was circulated to maintain the temperature of each block at 0°C (block *A*) and 35°C (block *B*). To interrupt the anterograde transport, the warm block (*B*) was placed proximal to the cold one (*A*) as shown in this figure. Inversely, the cold block was placed proximal to the warm one to interrupt the retrograde transport.

0.2 μl saline) was carefully injected into the ganglion (34) via a glass capillary (20–40 μm in tip width). At 1 h after injection, the above apparatus began to cool the right saphenous nerve locally and interrupt the fast anterograde transport of proteins labeled in cell bodies. After local cooling for 6 h, the mouse was killed, and the saphenous nerve (including L_2 ganglion) was dissected out. The nerve and ganglion were placed on an ice-cold plastic plate and cut into consecutive 3-mm segments. After being washed three times with 0.3 ml of ice-cold 5% (wt/vol) trichloroacetic acid, two times with 0.3 ml of absolute ethanol, and three times with 0.3 ml of N-hexan, each segment was air-dried and dissolved in 0.2 ml of Soluene 350 (Packard Instrument Co., Downers Grove, Ill.) in a vial by heating at 50°C for 2 h. After cooling, 3 ml of scintillation fluid (4 g of 2,5-diphenyloxazole and 0.25 g of 1,4-bis-[4-methyl-5-phenyloxazol-2-yl]benzene in 1 liter of toluene) was added to each vial. The vials were kept in a cool dark place for several hours before radioactivity was measured in a Packard model 3380 liquid-scintillation spectrometer.

Radioactive Tracer Experiment for Retrograde Transport

Under ether anesthesia, both right L_2 and L_3 dorsal root ganglia were exposed, and L-[^{35}S]methionine (100 μCi in 0.2 μl saline) was carefully injected into each ganglion. At 33 h after injection, the above apparatus began to cool the right saphenous nerve locally, interrupting retrograde transport. Our preliminary experiments showed that it took ~40–50 h for proteins labeled in ganglion cells to reach the cooled site by retrograde transport after turning back at the nerve endings. Because a small amount

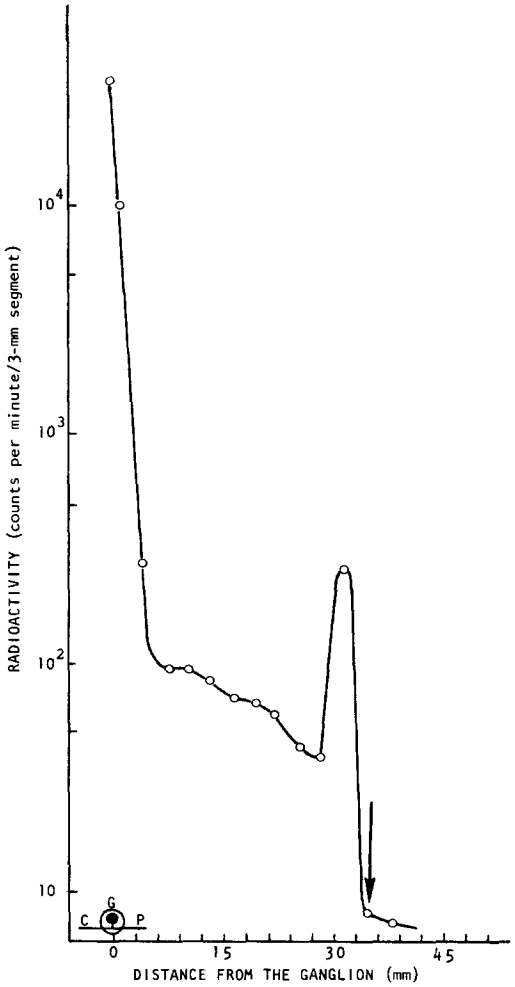

FIGURE 2 Blockade of the fast anterograde transport of proteins by local cooling. L-[^{14}C]leucine (0.4 μCi) was injected into the right L_2 dorsal root ganglion. At 33–35 mm distal from the dorsal root ganglion (arrow), the saphenous nerve was locally cooled (beginning 1 h after injection). *C*, central branch; *G*, ganglion, *P*, peripheral branch.

of the labeled proteins was shown to be transported retrogradely (2, 5, 18, 21), a large amount of L-[^{35}S]methionine was injected into two dorsal root ganglia, L_2 and L_3. After local cooling for 24 h, the mouse was killed and the saphenous nerve, including L_2 and L_3 ganglia, was dissected out. The nerve was cut into consecutive 3-mm segments, and the radioactivity of each segment was determined as described above.

Electron Microscopy

After local cooling of the saphenous nerve with the above apparatus for 10 h, the mouse was anesthetized with ether gas. Our preliminary experiments showed that at shorter cooling times (3 or 6 h) the morphological changes inside axons were not so dramatically shown as those at 10 h cooling, although the accumulated organelles in axons were morphologically the same. As control experiments, both aluminum blocks were circulated with warm (35°C) liquid for 10 h. Immediately after the blocks were removed, the saphenous nerve was exposed and fixed in situ for 20 min with 2% formaldehyde and 2.5% glutaraldehyde in 0.1 M sodium cacodylate buffer, pH 7.2. Then the saphenous nerve was dissected out, together with the muscle, and fixation was continued overnight at 4°C. The nerve was then cut into consecutive 1-mm long segments distally and proximally from the marked point. After being postfixed in cold 1% OsO_4 in the same buffer for 2 h, the segments were stained en bloc with 0.5% uranyl acetate for 2 h. They were then dehydrated in ethanol and embedded in Epon 812. Thin sections were cut, doubly stained with uranyl acetate and lead citrate, and then examined in a Hitachi 11-DS electron microscope at an accelerating voltage of 75 kV.

Tracer Experiment with HRP

Under ether anesthesia, the saphenous nerve just distal to the knee joint was carefully exposed and transected with a sharp razor blade. Soon after transection, the proximal cut end was treated with 2 mg of HRP powder (type VI, Sigma Chemical Company, St. Louis, Mo.), and the wound closed. In a control experiment, the cut end of the nerve was not treated. 90 min after administration of HRP, the saphenous nerve was locally cooled at the thigh level to interrupt retrograde transport. After local cooling for 10 h, the nerve was exposed and fixed in situ for 20 min with 1% formaldehyde and 1.25% glutaraldehyde in 0.1 M phosphate buffer, pH 7.2. The nerve was then dissected out and cut into consecutive 1-mm long segments, each of which was cut longitudinally into two pieces to open the perineurium. After being washed for 8 h with several changes of cold 0.1 M phosphate buffer, pH 7.2, containing 5% sucrose, the samples were first incubated for 1 h at room temperature in a freshly prepared solution of 5 mg 3,3′-diaminobenzidine (DAB) in 10 ml of 0.1 M phosphate buffer, pH 7.2, and then for an additional 1 h in the same solution containing 0.01% hydrogen peroxide for a second incubation (24). The samples were washed in the same buffer, postfixed in cold 2% OsO_4 in 0.1 M phosphate buffer for 1 h, and dehydrated in ethanol and embedded in Epon 812.

RESULTS

Radioactive Tracer Experiment

When the mouse saphenous nerve was cooled to interrupt the anterograde transport, ^{14}C-labeled proteins showed the characteristic pattern of distribution of radioactivity along the nerve. A sharp peak of radioactivity was demonstrated just proximal to the cooled site to such a degree that the labeled proteins accumulated only in one 3-mm-long segment (Fig. 2). The radioactivity of the distal side remained at the base-line value. The pattern of radioactivity with a prominent peak at the cooled region is essentially the same as that obtained from other methods, such as in ligation (see, for example, 45) and local cooling with excised nerves (17). In addition, this pattern differs from the normal flow pattern observed in un-

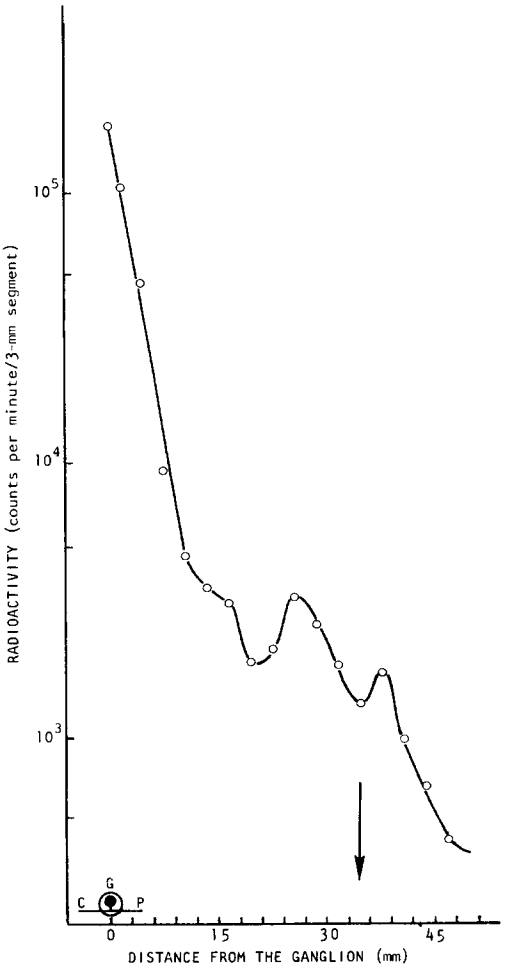

FIGURE 3 Blockade of the fast retrograde transport of proteins by local cooling. L-[^{35}S]methionine (100 μCi) was injected into both L_2 and L_3 dorsal root ganglia. At 33–35 mm distal from the dorsal root ganglia (arrow), the saphenous nerve was locally cooled for 24 h (beginning 33 h after injection) (see text). *C*, central branch; *G*, ganglion, *P*, peripheral branch.

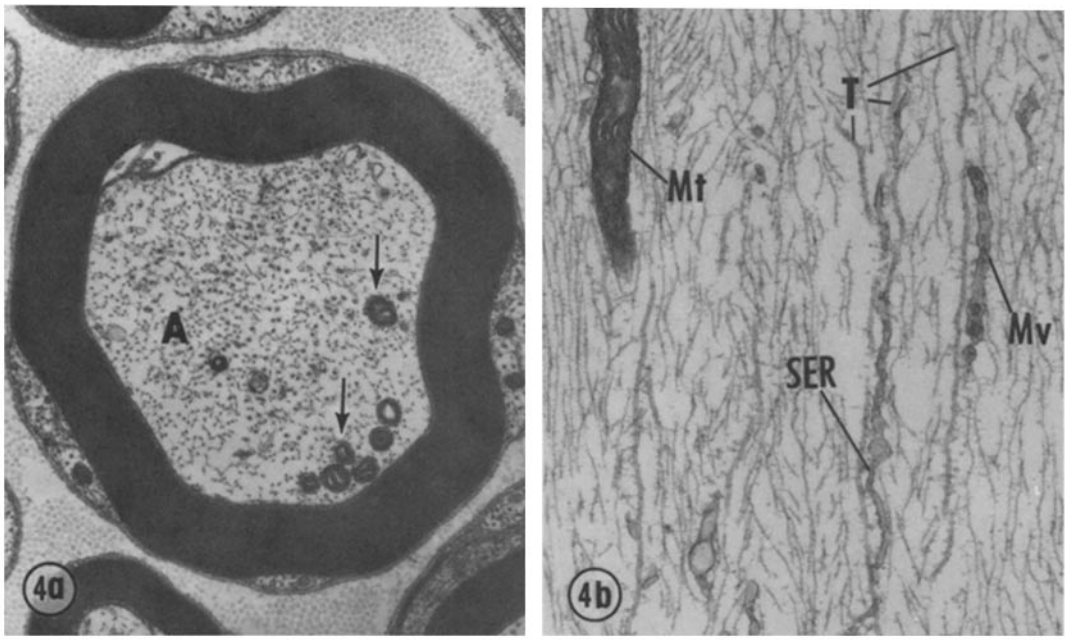

FIGURE 4 Myelinated axons in nontreated saphenous nerve. (*a*) Transverse section. The axoplasm (*A*) contains a small amount of membranous organelles, including mitochondria (arrows). × 16,000. (*b*) Longitudinal section. The membranous organelles in the axoplasm mainly comprise the axonal SER (*SER*), mitochondria (*Mt*), and large membranous bodies such as multivesicular bodies (*Mv*). These membranous organelles show an intimate spatial relationship with microtubules (*T*). × 24,000.

treated nerves in which the radioactivity front forms a weak peak. In our experiment, the nerve was locally cooled for 6 h (beginning 1 h after injection) at ~30 mm distal from the dorsal root ganglion. Because the rate of the fast transport has been estimated to be >200 mm/d in mammalian peripheral nerves (43), the activity front would have reached a point farther than 60 mm after 7 h if the nerve had not been cooled. The prominent peak observed can thus be interpreted to represent the blockade of fast anterograde transport.

After 24 h of local cooling to block retrograde transport, two peaks of radioactivity were visible: just distal and just proximal to the cooled site (Fig. 3). The flow pattern of the radioactivity resembles that reported in experiments for blockade of retrograde transport using ligation or transection (36, 45). Our preliminary experiments showed that the degree of peak formation at the distal region was dependent on the duration of local cooling. Hence, it is clear that this peak reflects the interruption of the retrograde transport. Furthermore, accumulation of the labeled proteins was also observed at the region ~6–12 mm proximal to the cooled site. Such accumulation can be regarded as a blockade of anterogradely transported proteins.

These radioactive tracer experiments were repeated four times, and the distribution patterns of radioactivity were reproducible. Thus, these results indicated that our local cooling method is effectively able to interrupt both fast anterograde and retrograde transport.

Electron Microscopic Observation

SAPHENOUS NERVE: At the level of local cooling, a mouse saphenous nerve was about 0.2 mm in diameter and ran through the subcutaneous tissue, accompanying small vessels. Electron microscopy showed that this nerve consisted of ~400 myelinated axons and >2,000 unmyelinated axons.

NONTREATED AXONS: The main membranous organelles in the axoplasm of the nontreated saphenous nerve were the axonal SER, mitochondria, and free large membranous bodies including multivesicular bodies (Fig. 4). The axonal SER appeared as pieces of slender tubules which were irregularly contoured, often beaded, and occasionally branched. These membranous organelles showed an intimate spatial relationship with microtubules.

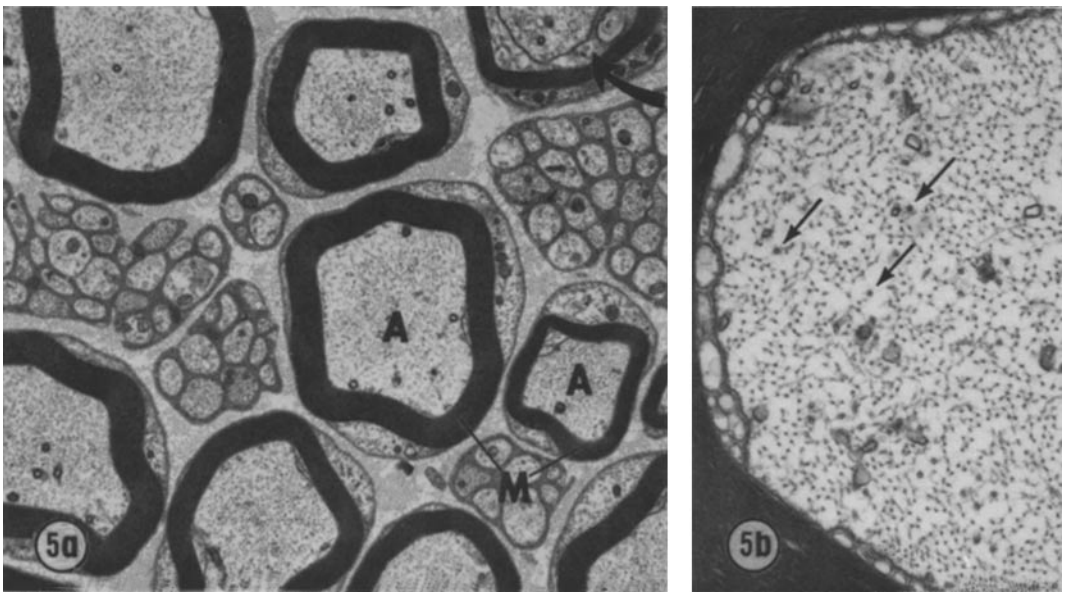

FIGURE 5 Transverse section of saphenous nerve at the cooled site. Cooling time, 10 h. (*a*) There is no detectable destruction of overall structures of axons (*A*), myelin sheaths (*M*), or other cells in the nerve. Arrow, Schmidt-Lantermann's incisure. × 5,500. (*b*) Microtubules (arrows) showed a significant decrease in number at the cooled site, though there were some variations in density among the axons. The possibility may not be excluded that some of the microtubules are re-formed before fixation takes effect. × 30,000.

ANTEROGRADE TRANSPORT BLOCKADE: After local cooling for 10 h to interrupt anterograde transport, 16 consecutive segments, each 1 mm long (8 segments proximal and 8 distal to the marked point), were examined by thin-section electron microscopy. The structural integrity of all segments, including the cooled segment, was well maintained (Fig. 5). No detectable destruction of overall structures of axons, myelin sheaths, or other cells in the nerves was observed. The characteristic feature was that the vesiculotubular membranous structures enormously increased in number inside both myelinated and unmyelinated axons only at the level of 0–2 mm proximal to the marked point (Fig. 6). In a given thin-section cut through this level, the number of vesiculotubular structures varied in different axons. Such differences may be due to the longitudinal irregularity of localization of these increased structures among the axons, which was not related to nodes of Ranvier. No accumulation of the membranous structures was discerned beyond 2 mm proximal to the cooled site. The localization of accumulated vesiculotubular structures coincided well with the prominent peak of radioactivity in the tracer experiment described above (Fig. 2). In the myelinated axons such vesiculotubular structures accumulated predominantly at the periphery beneath the axolemma in the internodal part (Fig. 7), whereas in the node of Ranvier the axons were distended, increasing their diameter and occasionally forming extensive bulges without any destruction of axolemma and myelin sheaths (Fig. 8). The incisures of Schmidt-Lantermann were not modified. The unmyelinated axons were similarly distended and filled with an accumulation of the same vesiculotubular structures (Fig. 9).

Such accumulated vesiculotubular membranous structures had a relatively uniform diameter of 50–80 nm with occasional branchings. In thin sections, these vesiculotubular structures varied in shape from spherical to elongated segments of tubules. Such tubules appeared to be blind-ended or even distended into spherical contours at both ends. The membrane profiles of these tubules were the same in both longitudinal and transverse sections of the axons. Hence, these tubular structures can be interpreted to be free segments rather than parts of the tubular network. The accumulation of vesiculotubular structures differed in appearance from the typical network of the axonal SER; however, these vesiculotubular structures were occasionally observed to be continuous with the axonal SER (Fig. 10). The continuity was also found

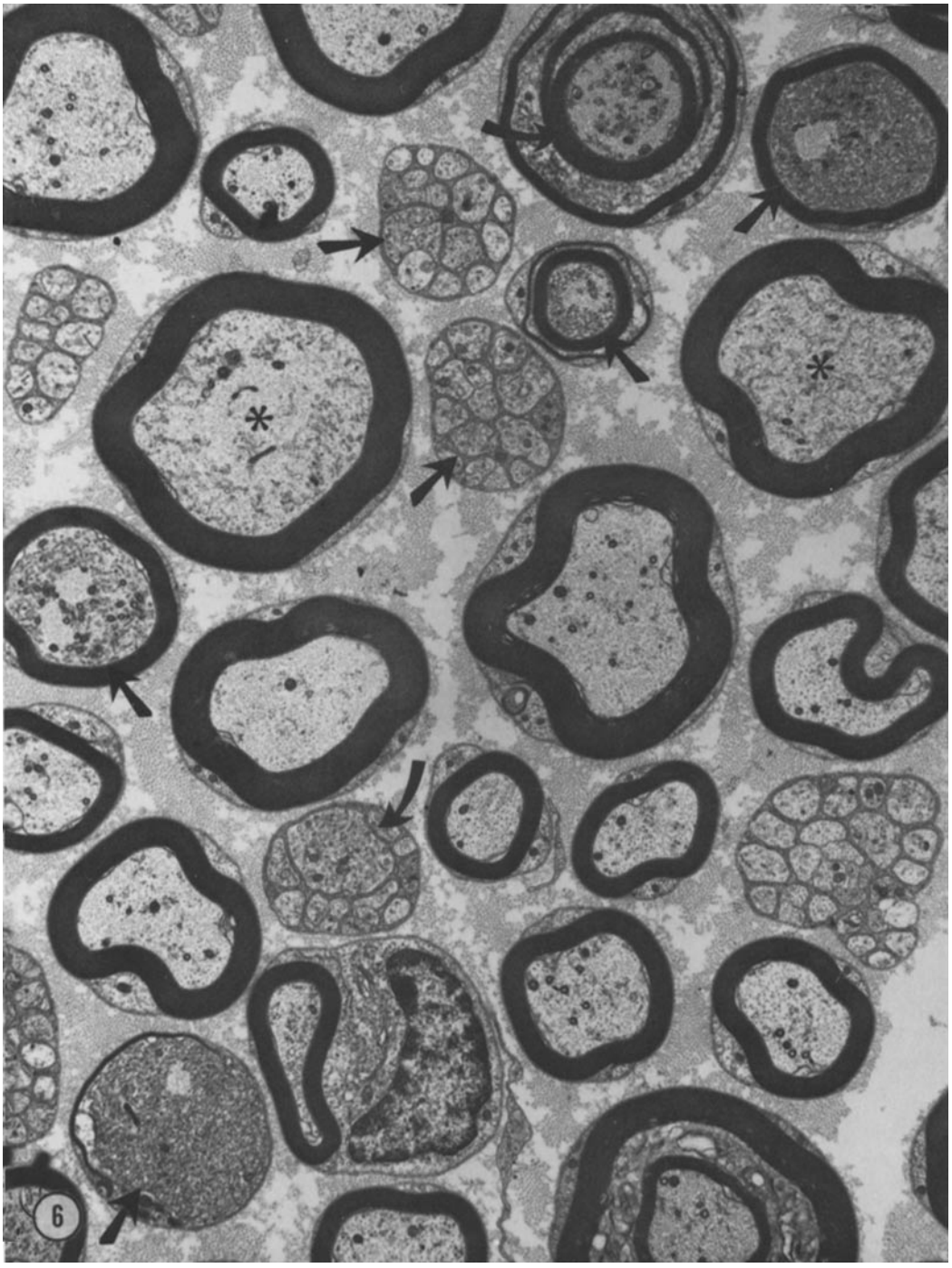

FIGURE 6 Transverse section of saphenous nerve just proximal to the cooled site in anterograde transport blockade. At this level of section many myelinated and unmyelinated axons exhibit the prominent accumulation of vesiculotubular membranous structures (arrows), whereas the other axons contain a moderate amount of such membranous structures (*). The structural integrity of all axons and myelin sheaths is well maintained. Cooling time, 10 h. × 6,000.

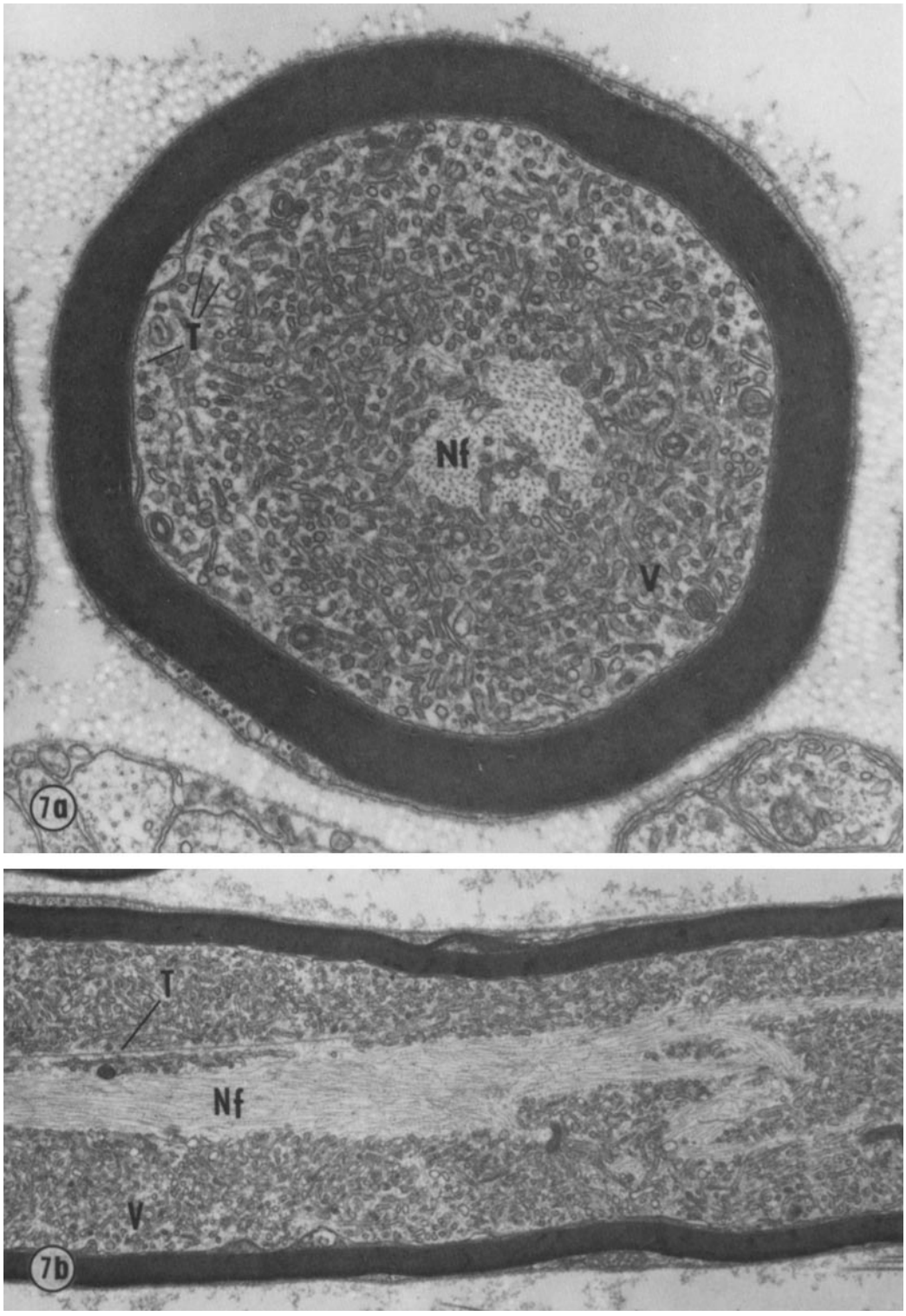

FIGURE 7 Internodal part of myelinated axons just proximal to the cooled site in anterograde transport blockade. Vesiculotubular membranous structures (*V*) accumulated predominantly at the periphery beneath the axolemma. A few microtubules (*T*) run through the accumulation of the membranous structures, whereas neurofilaments (*Nf*) are excluded from the membranous accumulation and form core bundles in the deep region. Cooling time, 10 h. (*a*) Transverse section. × 28,000. (*b*) Longitudinal section. × 12,000.

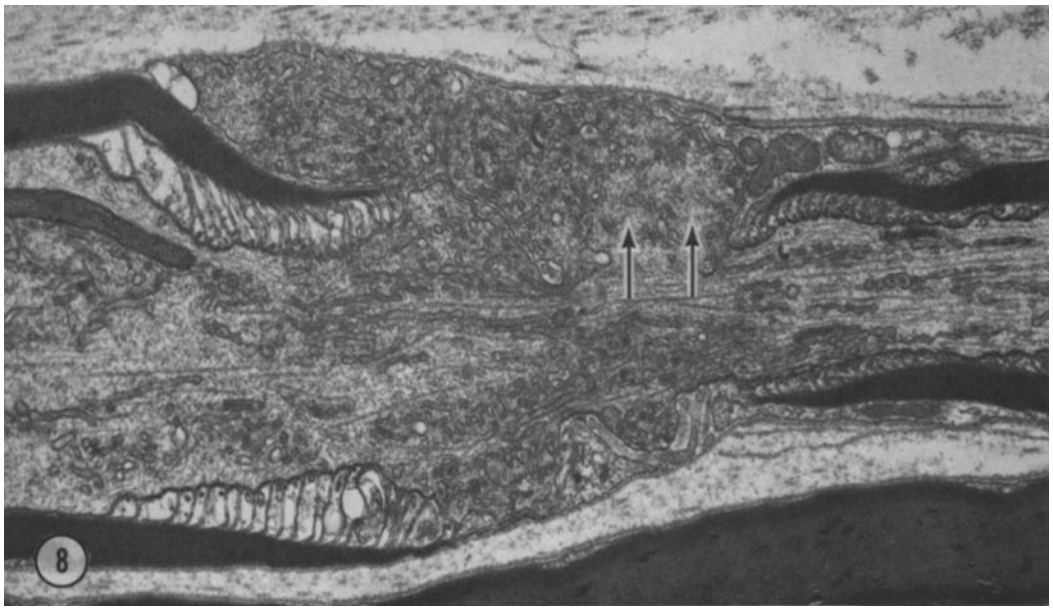

FIGURE 8 Node of Ranvier of myelinated axon just proximal to the cooled site in anterograde transport blockade. Vesiculotubular structures are seen accumulated at the nodal region, which is distended, occasionally forming an extensive bulge (arrows) without any destruction of the axolemma and myelin sheaths. Cooling time, 10 h. × 16,000.

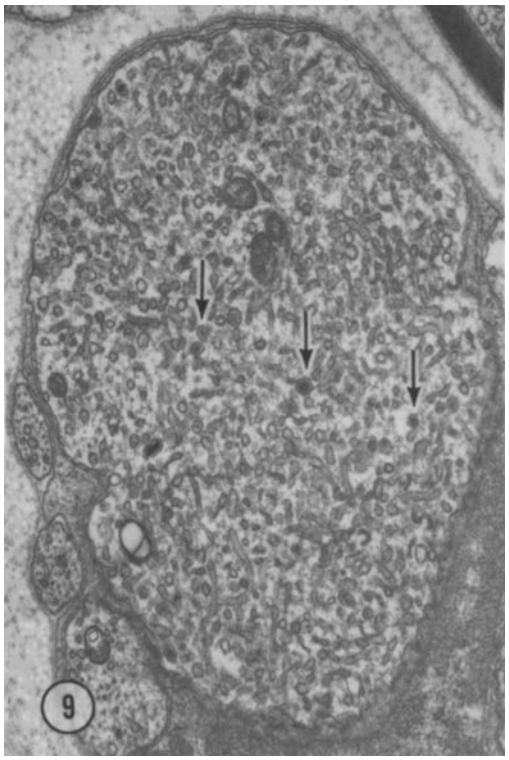

between these vesiculotubular structures and the axolemma, especially in unmyelinated axons (Fig. 11). The thickness of the membranes of the vesiculotubular structures was estimated to be the same as that of the axolemma. Although the vesiculotubular structures were studded with fine granular materials, there were no typical coated vesicles in the membrane accumulation. In farther proximal regions, where vesiculotubular structures were intermingled with the typical network of the axonal SER, the accumulation of membranous structures became less prominent. The mitochondria were seen scattered among the accumulated membranous structures, with no obvious increase in number, though there seemed to be a slight tendency for mitochondria to accumulate in the farther proximal region.

Inside the axons just proximal to the cooled site, both microtubules and neurofilaments decreased

FIGURE 9 Transverse section of unmyelinated axons just proximal to the cooled site in anterograde transport blockade. The axon is distended and filled with an accumulation of the vesiculotubular structures, among which dense-cored vesicles (arrows) are also found. Cooling time, 10 h. × 16,000.

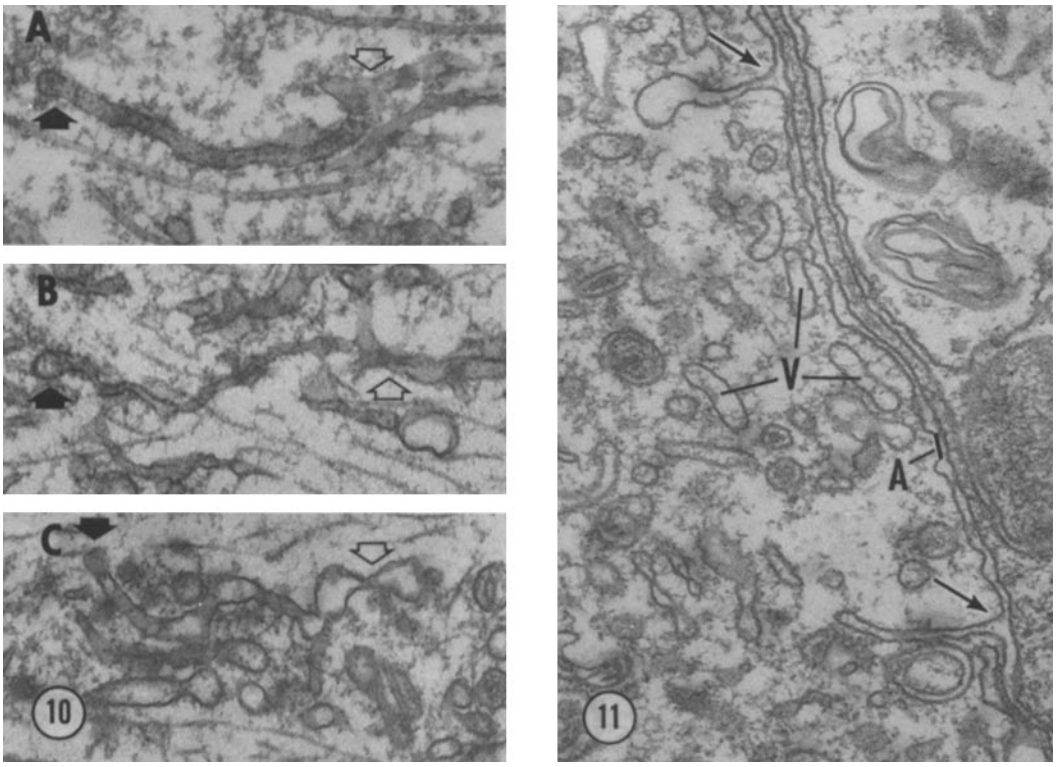

FIGURE 10 Membranous organelles in myelinated axons 1–2 mm proximal to the cooled site in anterograde transport blockade. The vesiculotubular structures with blind-ends (⬆) are continuous with the typical axonal SER (⇧) which is irregularly contoured, beaded, and branched as seen in three illustrations (*A*, *B*, and *C*). Cooling time, 10 h. × 52,000.

FIGURE 11 Transverse section of unmyelinated axon just proximal to the cooled site. The thickness of the membrane of the vesiculotubular structures (*V*) appears to be the same as that of the axolemma (*A*). Fine granular or filamentous materials increase in the axoplasm among the vesiculotubular structures. Some tubular structures are seen to be continuous with the axolemma (arrows). Cooling time, 10 h. × 70,000.

considerably in number. In thin sections, a few microtubules ran through the accumulation of the membranous structures, whereas neurofilaments were excluded from the membranous accumulation and formed core bundles in the deep region (Fig. 7). Interestingly, one could see an increased amount of fine granular or filamentous materials in the axoplasm where the membranous structures accumulated (Figs. 10 and 11).

In the region 2–4 mm proximal to the cooled site, the continuous network of the axonal SER was dramatically visible in 0.2-μm thick sections. Comparison with 0.2-μm sections of nontreated controls (Fig. 12) indicates that the network of the axonal SER at this level was more tightly packed (Fig. 13*a*). Furthermore, the thick sections more clearly showed the difference between the axonal SER network and the accumulated vesiculotubular structures (Fig. 13*b*). Thick sections of axons just proximal to the cooled site showed the accumulation of membranous structures. These were mainly in the form of tubular segments in more or less parallel array, although the SER network was still prominent in some axons (Fig. 14).

RETROGRADE TRANSPORT BLOCKADE: To interrupt the retrograde transport, the nerve was locally cooled for 10 h. Then all consecutive segments (each 1 mm long) were examined by electron microscopy. The structural integrity was well preserved. Morphological changes were observed in two regions: at the level of 0–2 mm distal to the marked point, many large membranous

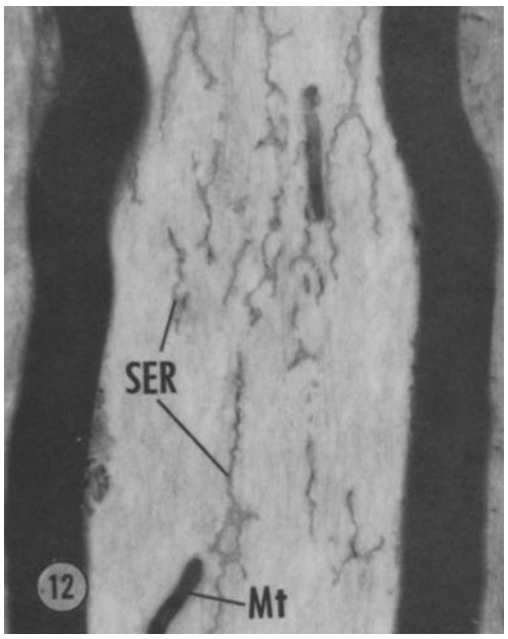

FIGURE 12 Thick section of selectively stained myelinated axon in nontreated saphenous nerve. The axonal membranous organelles were selectively stained according to the procedure previously used (56) as a modification of the original diaminobenzidine-potassium ferrocyanide method (58). 0.2-μm thick sections were examined without poststaining at an accelerating voltage of 75 kV. Axonal SER (*SER*) and mitochondria (*Mt*) are well contrasted. × 12,000.

bodies were found inside both myelinated and unmyelinated axons (Figs. 15 and 16); and at the level of 6–8 mm proximal to the marked point, vesiculotubular membranous structures similar to those in anterograde transport blockade were abundant. The number of large membranous bodies in the region distal to the marked point was smaller than the number of vesiculotubular structures observed in the anterograde transport blockade. No accumulation of these membranous bodies was detected beyond 2 mm distal to the marked point. The localization of accumulated vesiculotubular structures and large membranous bodies coincided with the peaks of radioactivity in the proximal and distal regions, respectively (Fig. 3).

Although large membranous bodies were composed of heterogeneous membranous structures of varying sizes, the main components of these structures were multivesicular bodies and lamellated bodies ranging from 100 to 500 nm (Figs. 15 and 16). Small amounts of the typical axonal SER were also observed among these membranous bodies. The large membranous bodies showed a tendency to accumulate predominantly at the periphery beneath the axolemma in myelinated axons in an accumulation pattern similar to that in the anterograde transport blockade. These bodies were never observed to be continuous with the axonal SER nor with the axolemma. At the node of Ranvier, the axoplasm was also filled with these membranous bodies, but no change in diameter of the axon was found, in contrast to the anterograde blockade.

Inside the axons just distal to the cooled site, microtubules did not appear to decrease in number. Thick sections (0.2 μm) revealed accumulations of large membranous organelles and a slight increase in axonal SER (Fig. 17).

In conclusion, an enormous number of vesiculotubular structures was consistently seen in the region where anterogradely transported proteins accumulated, whereas large membranous bodies increased in number in the region where the retrogradely transported proteins accumulated (Fig. 18). Both anterograde and retrograde transport blockade experiments were repeated more than five times, and the morphological changes described above were completely reproducible.

Tracer Experiment with HRP

To determine whether the large membranous bodies were transported retrogradely from the distal part of the axons, we administered HRP to the distal end of the saphenous nerve, and then locally cooled the nerve for 10 h. As a result, the activity of HRP was detected cytochemically in some of the membranous bodies accumulated in the region just distal to the cooled site (Fig. 19). At this level, no HRP activity was found in the endoneurium, indicating that the diffusion of the HRP was far behind the retrograde transport. Poststained thin sections showed that some of the multivesicular bodies and lamellated bodies were HRP positive. In the control experiments, no HRP-positive structure was observed in the axon.

DISCUSSION

Identification of Transported Organelles

The method described here was developed to study by electron microscope the interruption of fast axonal transport. By locally cooling the saphenous nerve in situ through the skin, the animal

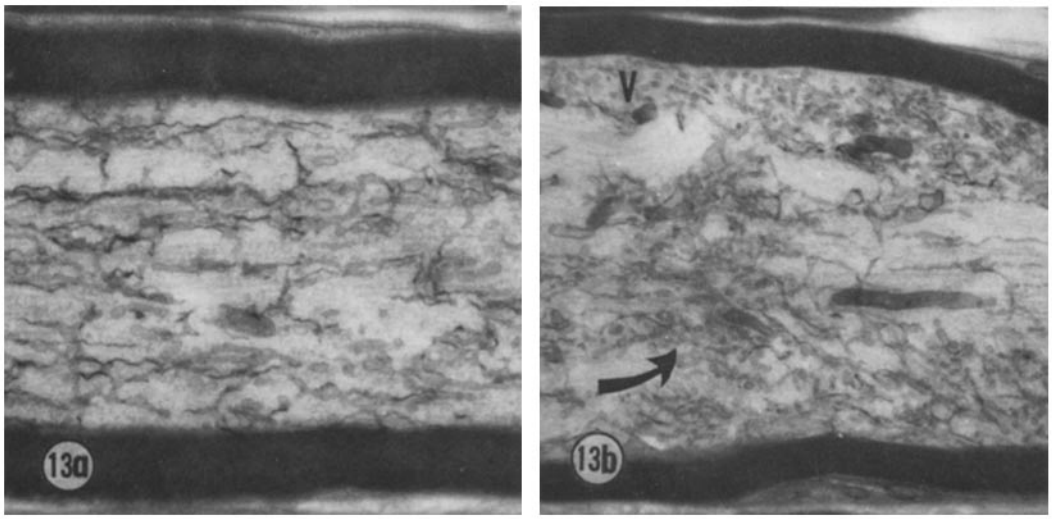
13a

V
13b

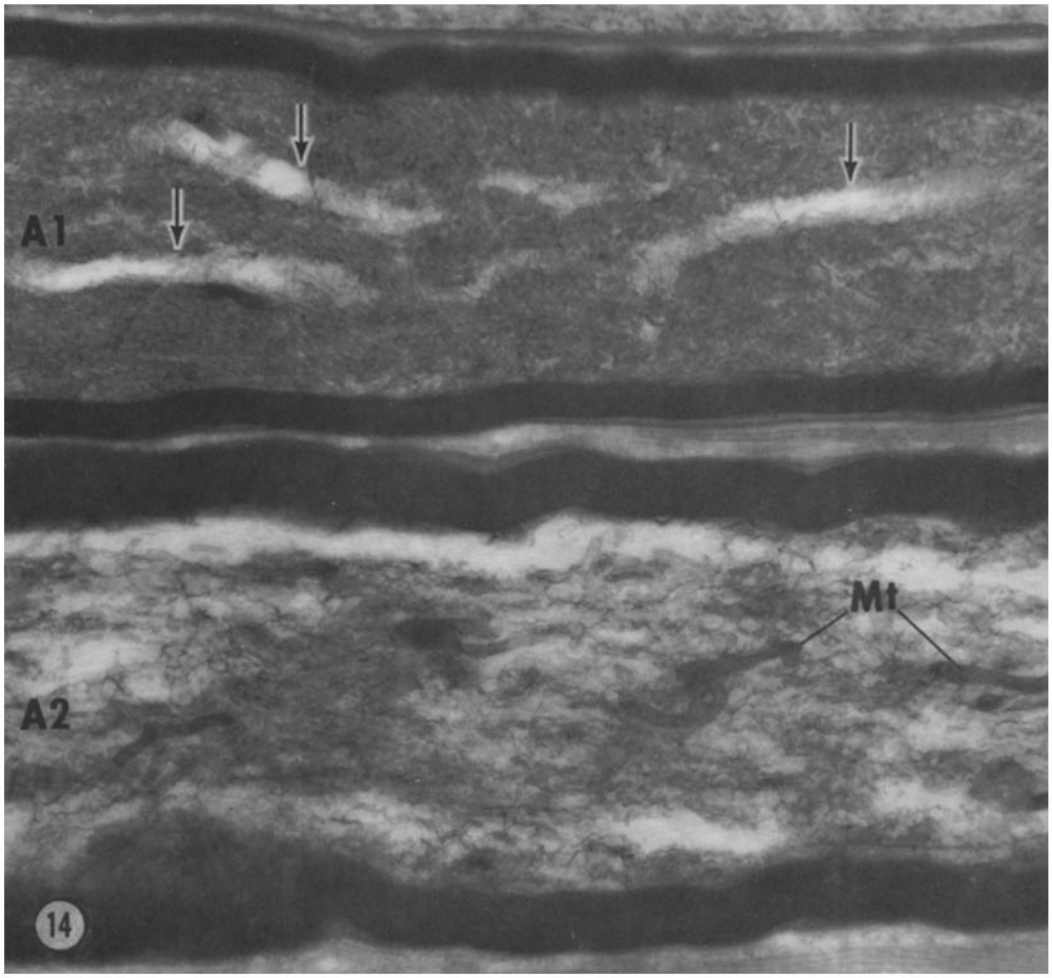
A1
Mt
A2
14

can be kept in a nonanesthetized state for a relatively long period of time. The nerve treated in this way retained its structural integrity without destruction at any level. Thus, this is a less damaging approach than other methods that have been used for similar purposes. Most of the organelles that accumulated, if not all, can be regarded as resulting from the interrupted axonal transport.

With this method, the nerve is cooled through the skin, so it is difficult to measure the exact temperature in the nerve itself. When monitored by an electric thermistor probe, the temperature of the subcutaneous tissue just beneath the cooled block was in the range of 0° to 5°C. Because below 10°C the rate of fast transport was shown to drop sharply in such homeothermal animals as cats (51) and rabbits (13), a temperature below 5°C should be sufficient to interrupt transport. The local temperature change at the border of the cooled site seemed to be reasonably large as judged by the biochemical analysis. Indeed, the membranous structures were accumulated within segments 1–2 mm long, although there was some longitudinal irregularity of the location of maximum accumulation of membranous structures among the axons. Such irregularity may be explained partly by the temperature difference, which may depend on the depth of axons within the nerve and on the proximity to the blood vessels.

Although we used the sensory nerve for the present study, fast axonal transport in sensory nerves has been demonstrated by biochemical analysis to be essentially the same as that in motor nerves (1). Our method offers a great advantage in fine structural analysis of experimental interruption of fast axonal transport. Furthermore, because this method permits recovery from the interruption simply by rewarming, it is possible to analyze the dynamic aspects of the transport.

The results obtained from both biochemical and morphological studies showed that our local cooling method successfully interrupted anterograde and retrograde axonal transports. The accumulation pattern of labeled proteins coincided well with that of membranous elements in both anterograde and retrograde transport blockade. Vesiculotubular membranous structures and large membranous bodies were seen densely packed where the anterogradely transported proteins and retrogradely transported proteins, respectively, accumulated. Furthermore, thick sections revealed that the network of the axonal SER, which was morphologically distinguishable from vesiculotubular structures, was tightly packed inside axons proximal to the cooled site. When the retrograde transport blockade was combined with the HRP tracer experiment, enzymatic activity in the axoplasm was demonstrated only in the large membranous bodies. Hence, we are led to propose that, besides mitochondria, the membranous components in the axon can be classified into two systems from the viewpoint of axonal transport: the axonal SER and vesiculotubular structures in the anterograde direction and free large membranous bodies in the retrograde direction. This proposal seems to be helpful in explaining many aspects of fast axonal transport so far elucidated.

Axonal SER in Fast Transport

In the present study, vesiculotubular membranous structures were shown to accumulate when the anterograde transport was experimentally blocked. The results suggest that the vesiculotubular structures were derived from the axonal SER, which were also seen packed inside axons proximal to the cooled site. The observation indicates that the axonal SER itself moves down the axon with its contents, excluding the possibility

FIGURE 13 Thick section of selectively stained myelinated axons 2–4 mm proximal to the cooled site in anterograde transport blockade. (*a*) The continuous network of the axonal SER is prominently visible as compared with the nontreated axon; 0.2-μm thick section. Cooling time, 10 h. × 16,000. (*b*) The vesiculotubular structures (*V*) are intermingled with the typical network of the axonal SER at this level of the axon (arrow); 0.2-μm thick section. Cooling time, 10 h. × 12,000.

FIGURE 14 Thick section of selectively stained myelinated axons just proximal to the cooled site in anterograde transport blockade. The accumulation of membranous structures inside axons (*A1*, *A2*) is dramatically shown in thick section. These were mainly in the form of vesiculotubular segments in more or less parallel array (see *A1*), although the SER network was still prominent in some axons (see *A2*). The regions indicated by arrows are considered to represent core bundles of neurofilaments (see also Fig. 7). *Mt*, mitochondria; 0.2-μm thick section. Cooling time, 10 h. × 12,000.

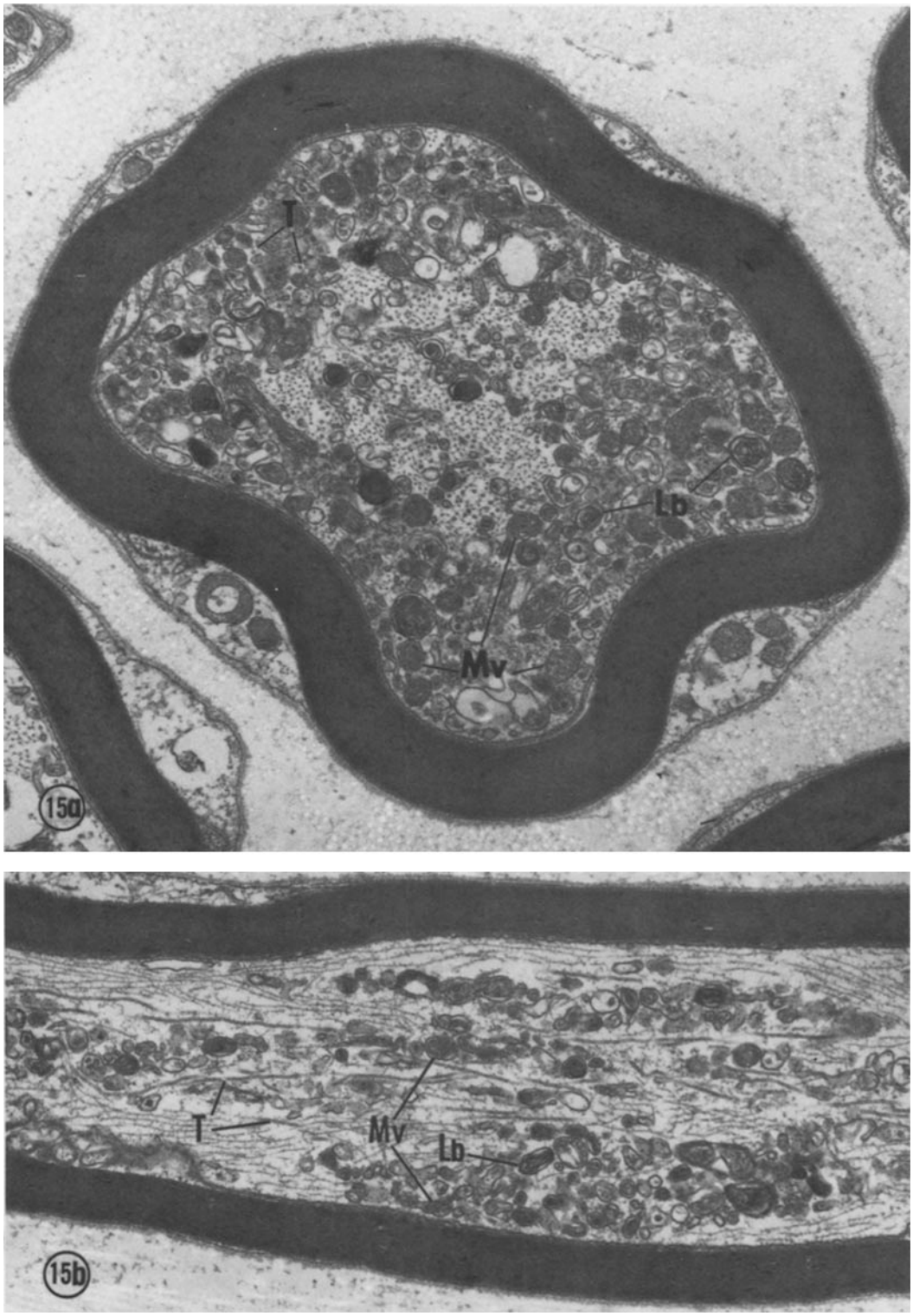

FIGURE 15 Internodal part of myelinated axon just distal to the cooled site in retrograde transport blockade. Large membranous bodies and mitochondria accumulated inside the axon. Large membranous bodies are composed of heterogeneous membranous structures, and the main components of these structures are multivesicular bodies (*Mv*) and lamellated bodies (*Lb*). *T*, microtubule. Cooling time, 10 h. (*a*) Transverse section. × 20,000. (*b*) Longitudinal section. × 20,000.

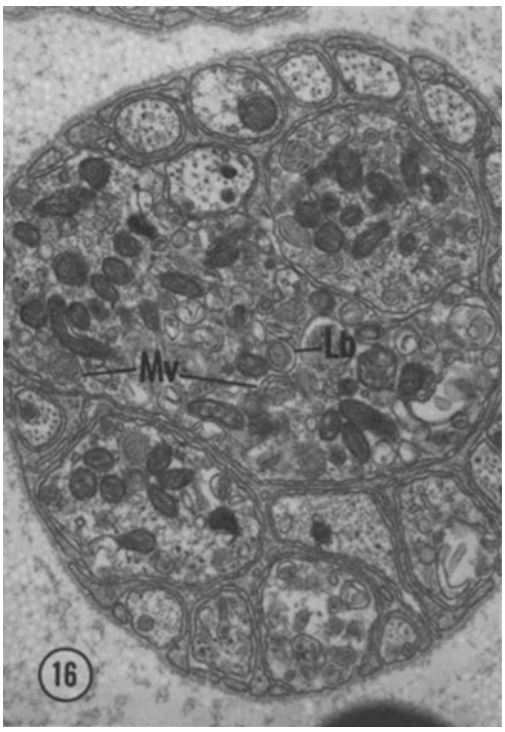

that the SER might serve as a pipe through which materials flow down. As previously shown (16, 56), the axonal SER forms a well-developed continuous network in the axoplasm. It seems unlikely that such a network of the SER moves fast as a whole through a densely packed fibrillar framework. Therefore, the most likely explanation is that in normal axons parts of the SER network may be pinched off into vesiculotubular structures, move down the axon, and fuse again with the network at any moment.

However, it is difficult to prove unequivocally that the vesiculotubular structures communicate with the axonal SER or are pinched off from it, only by morphological analysis. Alternatively, it is also possible that the vesiculotubular structures are present as such in normal axons and travel rapidly downstream in such low concentrations

FIGURE 16 Transverse section of unmyelinated axons just distal to the cooled site in retrograde transport blockade. The axon is distended and filled with an accumulation of mitochondria and large membranous bodies including multivesicular bodies (*Mv*) and lamellated bodies (*Lb*). Cooling time, 10 h. × 20,000.

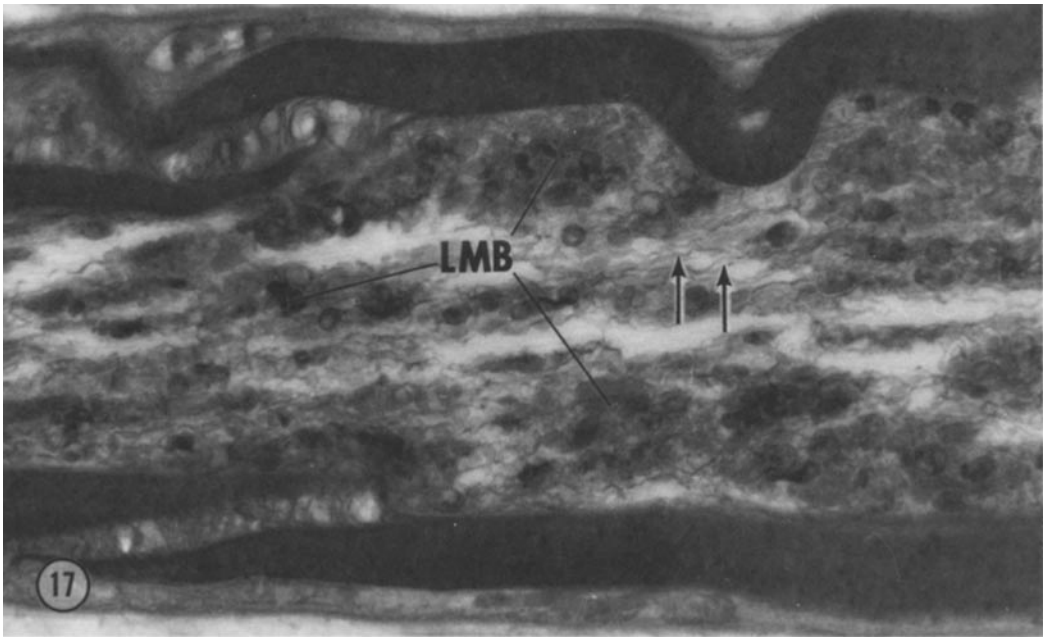

FIGURE 17 Thick section of selectively stained myelinated axon just distal to the cooled site in retrograde transport blockade. The axon is characterized by accumulated large membranous bodies (*LMB*). The SER showed a slight increase in amount (arrows); 0.2-μm thick section. Cooling time, 10 h. × 15,000.

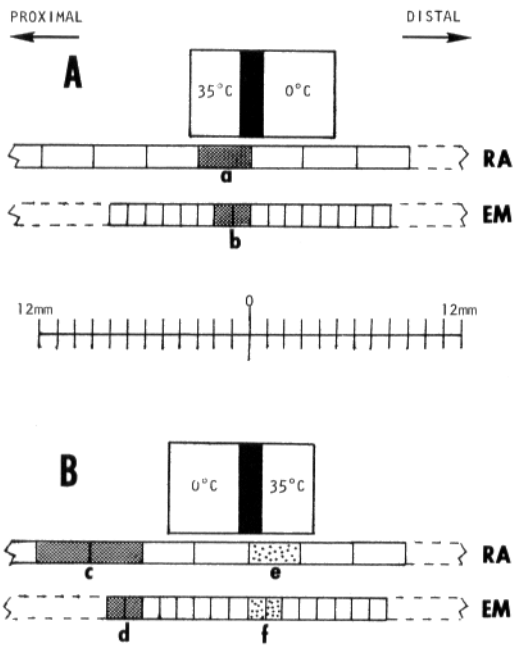

FIGURE 18 Summary of the results obtained from radioactive tracer experiments (*RA*) and electron microscopic observations (*EM*) in anterograde transport blockade (*A*) and in retrograde transport blockade (*B*). At the region where the anterogradely transported labeled proteins accumulated (in segments *a* and *c*), vesiculotubular membranous structures increased enormously in amount (in segments *b* and *d*). Where the retrogradely transported labeled proteins accumulated (in segment *e*), large membranous bodies increased in number (in segment *f*). Although the nerve proximal to the cooled site was not intentionally warmed in retrograde transport blockade (*B*), the anterogradely transported proteins and structures accumulated in segments *c* and *d*.

that they become noticeable only when their flow is dammed, and that the axonal SER network itself may move en masse more slowly.

At present, it is certain that the axonal SER are transported anterogradely, but additional studies are needed to determine whether the vesiculotubular structures are derived from the axonal SER or not.

Moving "Particles" in Light Microscopy

The movement of "particles" inside living nerve fibers has been directly observed through light microscopy. Although such movement has been noticed for many years (42), it is only recently that a quantitative analysis has been applied to this phenomenon (3, 7, 12, 20, 40, 41). Over 90% of the microscopically visible particles other than mitochondria move in a retrograde direction. These observations seem to disagree with biochemical evidence that indicates that the materials are transported more in an anterograde than in a retrograde direction (2, 5, 6, 18, 21, 43). This discrepancy may be explained when one considers that a large amount of the axonal SER is transported anterogradely and is too delicate to be detected under the light microscope. If the vesiculotubular structures are present in normal axons, they cannot be detected by light microscopy. In contrast, most of the large membranous bodies transported retrogradely fall well enough within the resolution of the light microscope. In the single case of cultured neurons, a moving particle was successfully fixed and examined by electron microscopy; it was identified as a large vesicle accompanied by a multivesicular body (7).

Conversely, the occurrence of a small number of anterogradely moving particles (12) may indicate that a few large membranous bodies can be also transported anterogradely.

Membranous Organelles Carrying HRP

Our observations revealed that the retrograde transport of HRP was demonstrated only in large

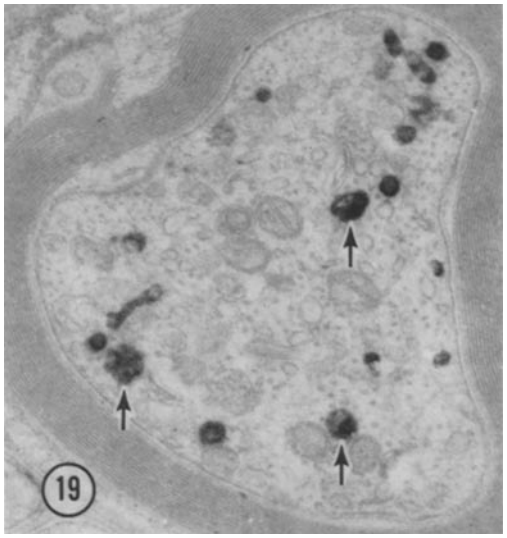

FIGURE 19 Transverse section of myelinated axon just distal to the cooled site in retrograde transport blockade after administration of HRP to the distal end of the saphenous nerve. The activity of HRP is detected cytochemically in some of the large accumulated membranous bodies (arrows). Cooling time, 10 h. × 30,000.

membranous bodies. The membranous organelles retrogradely carrying HRP have been studied in detail by LaVail and LaVail (38). In addition to vesicles, multivesicular bodies, and cup-shaped organelles, small tubules were also HRP positive. Judged by their morphological characteristics and by our retrograde transport blockade experiments, those structures, including the small tubules, may belong to the system of large membranous bodies classified in our study but not to the axonal SER. Birks et al. (4) analyzed pinocytosis in cultured chick embryo sympathetic ganglion cells and classified intraaxonal membranous organelles into axonal SER and blind-ended tubules (including multivesicular bodies). In their study, exogenous ferritin or thorium dioxide was incorporated only inside the blind-ended tubules, never inside the axonal SER. It may be concluded that the HRP is retrogradely transported by free large membranous bodies, not by the axonal SER.

The situation seems to be complicated by discovery of the anterograde transport of HRP administered at the region of the perikarya (11, 27, 38, 47, 52, 55). As the anterograde transport of HRP was demonstrated in the membrane-bounded structures seeming to have no morphological characteristics of the axonal SER, it is likely that these membranous organelles may belong to the system of large membranous bodies. If this is the case, the large membranous bodies also can move anterogradely, but in much smaller numbers (38). Alternatively, if the vesiculotubular membranous structures are present in normal axons, it is possible that these HRP-positive structures may belong to the vesiculotubular structures.

In this study, we developed a new local cooling method which offered a great advantage in fine structural analysis of experimental interruption of fast axonal transport. By this method, furthermore, it was confirmed that there were bidirectional movements of membranous organelles in the axons, and that largely different membranous systems were engaged in transport in different directions. Hence, axonal transport can be a useful model for the mechanism of intracellular movement of the membranous organelles in a variety of cell types.

We wish to thank Dr. Yoshiaki Komiya of the Institute of Brain Research, University of Tokyo, for his collaboration in radioactive tracer experiments and for his helpful discussions. We also wish to thank Prof. Eichi Yamada and Prof. Masanori Kurokawa of the University of Tokyo, for valuable discussions throughout this work.

Received for publication 29 May 1979, and in revised form 16 September 1979.

REFERENCES

1. ABE, T., T. HAGA, and M. KUROKAWA. 1973. Rapid transport of phosphatidylcholine occurring simultaneously with protein transport in the frog sciatic nerve. *Biochem. J.* **136**:731–740.
2. ABE, T., T. HAGA, and M. KUROKAWA. 1974. Retrograde axoplasmic transport: its continuation as anterograde transport. *FEBS (Fed. Eur. Biochem. Soc.) Lett.* **47**:272–275.
3. BERLINROOD, M., S. M. MCGEE-RUSSELL, and R. D. ALLEN. 1972. Patterns of particle movement in nerve fibres in vitro—an analysis by photokymography and microscopy. *J. Cell Sci.* **11**:875–886.
4. BIRKS, R. I., M. C. MACKEY, and P. R. WELDON. 1972. Organelle formation from pinocytotic elements in neurites of cultured sympathetic ganglia. *J. Neurocytol.* **1**:311–340.
5. BISBY, M. A. 1976. Orthograde and retrograde axonal transport of labeled protein in motoneurons. *Exp. Neurol.* **50**:628–640.
6. BRAY, J. J., C. M. KON, and B. M. BRECKENRIDGE. 1971. Reversed polarity of rapid axonal transport in chicken motoneurons. *Brain Res.* **33**:560–564.
7. BREUER, A. C., C. N. CHRISTIAN, M. HENKART, and P. G. NELSON. 1975. Computer analysis of organelle translocation in primary neuronal cultures and continuous cell lines. *J. Cell Biol.* **65**:562–576.
8. BRIMIJOIN, S. 1975. Stop-flow: a new technique for measuring axonal transport, and its application to the transport of dopamine-β-hydroxylase. *J. Neurobiol.* **6**:379–394.
9. BYERS, M. R. 1974. Structural correlates of rapid axonal transport: evidence that microtubules may not be directly involved. *Brain Res.* **75**: 97–113.
10. CANCALON, P., and L. M. BEIDLER. 1975. Distribution along the axon and into various subcellular fractions of molecules labeled with [^{3}H]leucine and rapidly transported in the garfish olfactory nerve. *Brain Res.* **89**:225–244.
11. COLMAN, D. R., F. SCALIA, and E. CABRALES. 1976. Light and electron microscopic observations on the anterograde transport of horseradish peroxidase in the optic pathway in the mouse and rat. *Brain Res.* **102**: 156–163.
12. COOPER, P. D., and R. S. SMITH. 1974. The movement of optically detectable organelles in myelinated axons of *Xenopus laevis*. *J. Physiol. (Lond.).* **242**:77–97.
13. COSENS, B., D. THACKER, and S. BRIMIJOIN. 1976. Temperature-dependence of rapid axonal transport in sympathetic nerves of rabbit. *J. Neurobiol.* **7**:339–354.
14. DI GIAMBERARDINO, L., G. BENNETT, H. L. KOENIG, and B. DROZ. 1973. Axonal migration of protein and glycoprotein to nerve endings. III. Cell fraction analysis of chicken ciliary ganglion after intracerebral injection of labeled precursors of proteins and glycoproteins. *Brain Res.* **60**:147–159.
15. DROZ, B., H. L. KOENIG, and L. DI GIAMBERARDINO. 1973. Axonal migration of protein and glycoprotein to nerve endings. I. Radioautographic analysis of the renewal of protein in nerve endings of chicken ciliary ganglion after intracerebral injection of [^{3}H]lysine. *Brain Res.* **60**:93–127.
16. DROZ, B., A. RAMBOURG, and H. L. KOENIG. 1975. The smooth endoplasmic reticulum: structure and role in the renewal of axonal membrane and synaptic vesicles by fast axonal transport. *Brain Res.* **93**:1–13.
17. EDSTRÖM, A., and M. HANSON. 1973. Temperature effects on fast axonal transport of proteins in vitro in frog sciatic nerves. *Brain Res.* **58**:345–354.
18. EDSTRÖM, A., and M. HANSON. 1973. Retrograde axonal transport of proteins in vitro in frog sciatic nerves. *Brain Res.* **61**:311–320.
19. ELAM, J. S., and B. W. AGRANOFF. 1971. Transport of proteins and sulfated mucopolysaccharides in the goldfish visual system. *J. Neurobiol.* **2**:379–390.
20. FORMAN, D. S., A. L. PADJEN, and G. R. SIGGINS. 1977. Axonal transport of organelles visualized by light microscopy: cinemicrographic and computer analysis. *Brain Res.* **136**:197–213.
21. FRIZELL, M., and J. SJÖSTRAND. 1974. Retrograde axonal transport of rapidly migrating proteins in the vagus and hypoglossal nerves of the rabbit. *J. Neurochem.* **23**:651–657.
22. GRAFSTEIN, B., D. S. FORMAN, and B. S. MCEWEN. 1972. Effects of temperature on axonal transport and turnover of protein in goldfish optic system. *Exp. Neurol.* **34**:158–170.
23. GRAFSTEIN, B., J. A. MILLER, R. W. LEDEEN, J. HALEY, and S. C.

SPECHT. 1975. Axonal transport of phospholipid in goldfish optic system. *Exp. Neurol.* **46**:261–281.
24. GRAHAM, R. C., JR., and M. J. KARNOVSKY. 1966. The early stages of absorption of injected horseradish peroxidase in the proximal tubule of mouse kidney: ultrastructural cytochemistry by a new technique. *J. Histochem. Cytochem.* **14**:291–302.
25. GROSS, G. W. 1973. The effect of temperature on the rapid axoplasmic transport in C-fibers. *Brain Res.* **56**:359–363.
26. HANSON, M. 1978. A new method to study fast axonal transport in vivo. *Brain Res.* **153**:121–126.
27. HANSSON, H. A. 1973. Uptake and intracellular bidirectional transport of horseradish peroxidase in retinal ganglion cells. *Exp. Eye Res.* **16**: 377–388.
28. HENDRICKSON, A. E. 1972. Electron microscopic distribution of axoplasmic transport. *J. Comp. Neurol.* **144**:381–398.
29. HESLOP, J. P. 1975. Axonal flow and fast transport in nerves. Adv. *Comp. Physiol. Biochem.* **6**:75–163.
30. HESLOP, J. P., and E. A. HOWES. 1972. Temperature and inhibitor effects on fast axonal transport in a molluscan nerve. *J. Neurochem.* **19**: 1709–1716.
31. HOFFMAN, P. N., and R. J. LASEK. 1975. The slow component of axonal transport. Identification of major structural polypeptides of the axon and their generality among mammalian neurons. *J. Cell Biol.* **66**:351–366.
32. KARLSSON, J.-O., and J. SJÖSTRAND. 1971. Rapid intracellular transport of fucose-containing glycoproteins in retinal ganglion cells. *J. Neurochem.* **18**:2209–2216.
33. KERKUT, G. A. 1975. Axoplasmic transport. *Comp. Biochem. Physiol.* **51A**:701–704.
34. KOMIYA, Y., and M. KUROKAWA. 1978. Asymmetry of protein transport in two branches of bifurcating axons. *Brain Res.* **139**:354–358.
35. KRISTENSSON, K., and Y. OLSSON. 1971. Retrograde axonal transport of protein. *Brain Res.* **29**:363–365.
36. LASEK, R. J. 1967. Bidirectional transport of radioactively labeled axoplasmic components. *Nature (Lond.).* **216**:1212–1214.
37. LASEK, R. J., and P. N. HOFFMAN. 1976. The neuronal cytoskeleton, axonal transport and axonal growth. *In* Cell Motility. Goldman, Pollard, and Rosenbaum, editors. Cold Spring Harbor Laboratory, Cold Spring Harbor, N. Y. **3**:1021–1049.
38. LAVAIL, J. H., and M. M. LAVAIL. 1974. The retrograde intraaxonal transport of horseradish peroxidase in the chick visual system: a light and electron microscopic study. *J. Comp. Neurol.* **157**:303–358.
39. LAVAIL, M. M., and J. H. LAVAIL. 1975. Retrograde intraaxonal transport of horseradish peroxidase in retinal ganglion cells of the chick. *Brain Res.* **85**:273–280.
40. LEESTMA, J. E. 1976. Velocity measurements of particulate neuroplasmic flow in organized mammalian CNS tissue cultures. *J. Neurobiol.* **7**:173–183.
41. LEESTMA, J. E., and S. S. FREEMAN. 1977. Computer-assisted analysis of particulate axoplasmic flow in organized CNS tissue cultures. *J. Neurobiol.* **8**:453–467.
42. LUBINSKA, L. 1975. On axoplasmic flow. *Int. Rev. Neurobiol.* **17**:241–296.
43. LUBINSKA, L., and S. NIEMIERKO. 1971. Velocity and intensity of bidirectional migration of acetylcholinesterase in transected nerves. *Brain Res.* **27**:329–342.
44. MCEWEN, B. S., D. S. FORMAN, and B. GRAFSTEIN. 1971. Components of fast and slow axonal transport in the goldfish optic nerve. *J. Neurobiol.* **2**:361–377.
45. MIANI, N. 1964. Proximo-distal movement of phospholipid in axoplasm of the intact and regenerating neurons. *Prog. Brain Res.* **13**:115–126.
46. MORI, H., Y. KOMIYA, and M. KUROKAWA. 1979. Slowly migrating axonal polypeptides. Inequalities in their rate and amount of transport between two branches of bifurcating axons. *J. Cell Biol.* **82**:174–184.
47. NAUTA, H. J. W., I. R. KAISERMAN-ABRAMOF, and R. J. LASEK. 1975. Electron microscopic observations of horseradish peroxidase transported from the caudoputamen to the substantia nigra in the rat: possible involvement of the agranular reticulum. *Brain Res.* **85**:373–384.
48. OCHS, S. 1971. Characteristics and a model for fast axoplasmic transport in nerve. *J. Neurobiol.* **2**:331–345.
49. OCHS, S. 1972. Fast transport of materials in mammalian nerve fibers. *Science (Wash. D. C.).* **176**:252–260.
50. OCHS, S. 1974. Systems of material transport in nerve fibers (axoplasmic transport) related to nerve function and trophic control. Ann. N. Y. Acad. Sci. **228**:202–223.
51. OCHS, S., and C. SMITH. 1975. Low temperature slowing and cold-block of fast axoplasmic transport in mammalian nerves in vivo. *J. Neurobiol.* **6**:85–102.
52. REPÉRANT, J. 1975. The orthograde transport of horseradish peroxidase in the visual system. *Brain Res.* **85**:307–312.
53. SCHMITT, F. O. 1968. Fibrous proteins—neuronal organelles. *Proc. Natl. Acad. Sci. U. S. A.* **60**:1092–1101.
54. SCHONBACH, J., CH. SCHONBACH, and M. CUÉNOD. 1971. Rapid phase of axoplasmic flow and synaptic proteins: an electron microscopical autoradiographic study. *J. Comp. Neurol.* **141**:485–498.
55. SOTELO, C., and D. RICHE. 1974. The smooth endoplasmic reticulum and the retrograde and fast orthograde transport of horseradish peroxidase in the nigro-striate-nigral loop. *Anat. Embryol.* **146**:209–218.
56. TSUKITA, S., and H. ISHIKAWA. 1976. Three-dimensional distribution of smooth endoplasmic reticulum in myelinated axons. *J. Electron Microsc.* **25**:141–149.
57. TSUKITA, S., and H. ISHIKAWA. 1979. Morphological evidence for the involvement of the smooth endoplasmic reticulum in axonal transport. *Brain Res.* **174**:315–318.
58. WAUGH, R. A., J. R. SOMMER, and L. D. PEACHEY. 1974. Cardiac sarcoplasmic reticulum: distribution and ultrastructure revealed by selective staining. *Circulation.* **50**(Suppl. III):13 (Abstr.).